

# APPLICATION OF THE RIETVELD METHOD TO THE ANALYSIS OF XRD DATA OF CORROSION DEPOSITS FORMED IN EQUIPMENT PARTS OF REFINERIES AND GAS PLANTS

*Husin Sitepu & Rasha A. Al-Ghamdi*

*Research and Development Center, Saudi Aramco, Dhahran, Saudi Arabia*

---

Received: 10 Jul 2018

Accepted: 01 Aug 2018

Published: 31 Aug 2018

---

## ABSTRACT

*This article reports the application of the Rietveld method to the quantitative analysis of corrosion deposits which is certainly an important industrial application, and an educational paper on the analysis of such deposits is worthwhile. The basic premise of this paper - that crystallographic preferred orientation can affect the results of a quantitative analysis - is important, and worth discussing. Examples of (i) structure, texture characterization and quantitative analysis of iron oxide corrosion products from the boiler tube equipment in gas plant in the form of magnetite [Fe<sub>3</sub>O<sub>4</sub>], hematite [Fe<sub>2</sub>O<sub>3</sub>], goethite [FeO(OH)], and formation material normally found in the sandstone or sand in the form of quartz [SiO<sub>2</sub>] and (ii) quantitative phase analysis of synthetic mixtures of barite, quartz and hematite and (iii) quantitative phase analysis of sludge deposits that were collected from the equipment parts in a refinery, which are very useful in quantitative phase analysis by Rietveld method. Key information is not just the phase concentrations, but the lattice parameters (which can reflect composition) and information derived from the profile parameters and the preferred orientation. All aspects of the microstructure are worth discussing. Magnetite and hematite are especially prone to the preferred orientation, and so would be worth including in the samples discussed. Knowing accurately which phase are involved along with the structure, texture and compositions for each of the identified phases in the scale formation and corrosion deposits can guide the field engineers at the refinery and gas plants to facilitate the efficient cleaning of the equipment by drawing up the right procedures and taking preventive action to stop the generation of those particular deposits.*

**KEYWORDS:** *Rietveld Method, XRD, Texture, Quantitative Phase Analysis, Structural Refinement*

## INTRODUCTION

The corrosion deposits in the form of iron oxide corrosion products are generated in the particular equipment in oil and gas plants can cause major operational problems and would have to be temporary shutdown refinery and gas plants<sup>1</sup>. Therefore, the Research and Development Center (R&DC) sought to accurately and quickly investigate the failure of equipment due to the specific carbonate scale and/or corrosion deposits products and provide support to the engineers at refinery and gas plant by firstly identifying the nature and source of the phases of deposits being accumulated<sup>2</sup>. For example, X-ray powder diffraction (XRD) data of deposits can be quickly and accurately identified of the nature of the materials such as

- Iron oxide corrosion products —(i) at high temperature, magnetite [Fe<sub>3</sub>O<sub>4</sub>] corrosion product formed and it will coat the iron/steel to prevent oxygen to reach underlying metal, (ii) at low temperature, there are mostly lepidocrocite formed and with time it transformed into most stable goethite [FeOOH], and (iii) in marine environment, akaganeite [FeOOH] product formed,
- Iron sulfide corrosion product types —greigite [Fe<sub>3</sub>S<sub>4</sub>], pyrite [FeS<sub>2</sub>], marcasite [FeS<sub>2</sub>], mackinawite [FeS<sub>0.9</sub>], and pyrrhotite [Fe<sub>7</sub>S<sub>8</sub>]—are the pyrophoric iron sulfide in the form of pyrrhotite [FeS] results from the corrosive action of sulfur [S] or sulfur compound [H<sub>2</sub>S] on the iron (steel) and moisture,
- Formation materials—found formally in the sandstone or sand in the form of silicon oxide with the mineral name quartz (SiO<sub>2</sub>), and
- Cementing materials —ettringite [Ca<sub>6</sub>Al<sub>2</sub>(SO<sub>4</sub>)<sub>3</sub>(OH)<sub>12</sub>]<sup>2</sup>].

The accurate phase identification result of the XRD data of deposits on the very small quantities of inorganic materials (non-hydrocarbon) in the forms of carbonate scale or corrosion products is vital to facilitate efficient chemical cleaning of the equipment in refineries and gas plants and prevent the future occurrences to stop the generation of deposits<sup>2</sup>. Unfortunately, when analysts at the industry, especially those who do not have strongly X-ray crystallography background, perform a quantitative phase analysis<sup>3-7</sup> of the identified phases of the XRD data of deposits using the Rietveld method<sup>8-14</sup>, they frequently assume that the deposits formed in oil and gas plants are randomly oriented. In practice, all crystalline materials reveal some degree of crystallographic preferred orientation (i.e., the texture of crystalline materials) that can be caused serious systematic errors in phase composition analysis and also in crystal structure determination of powder diffraction data<sup>15-23</sup>.

In this paper, when all the phases of XRD data of deposits are identified accurately by the combined software package PANalytical High Score Plus<sup>13</sup> (X'Pert HighScore Plus Version 3.0e PANalytical Inc.) with the International Centre for Diffraction Data (ICDD) of the powder diffraction file (PDF-4+) database of the standard reference materials, the GSAS Rietveld software<sup>24</sup> will then be used to perform the

- Crystal structures, crystallographic preferred orientations refinement<sup>15-23</sup> and quantitative phase analysis<sup>3-7</sup> of XRD data of corrosion deposits from the boiler;
- Quantitative phase analysis of XRD data of synthetic mixtures of drilling mud in the form of barium sulfate (87 wt% of barite-BaSO<sub>4</sub>), formation material in the form of silicon oxide (8 wt% of quartz-SiO<sub>2</sub>) and iron oxide corrosion products (5 wt% of hematite-Fe<sub>2</sub>O<sub>3</sub>); and
- Quantitative phase analysis of sludge deposits that were collected from the equipment parts in a refinery.

In performing the refinement for quantitative analysis<sup>3-7</sup>, Rietveld method<sup>8-14</sup> which adjusts the refinable parameters until the best fit of the entire calculated pattern to the entire measured pattern is achieved does not require measurement of calibration data nor the use of an internal standard. However, Rietveld method<sup>8-14</sup> requires the crystallographic information file (e.g., crystal structures) that has closely to each of the identified phases. This preferred orientation is fully described by the orientation distribution function<sup>15</sup>, which is a mapping of the probability of each possible grain-orientation with respect to the macroscopic sample frame<sup>15-23</sup>. The objective of this paper is to discuss the influence of the different parameters

(crystal structure, crystallographic preferred orientation)involved in the Rietveld refinement and describe the most recent quantitative XRD studies on scale deposits and corrosion deposits products.

In the GSAS Rietveld refinement program<sup>24</sup>, a mathematical method is developed that calculates an intensity,  $Y_c$ , at every point in the pattern, i.e.,

$$Y_c = \sum_h SKF_h^2 P(\Delta T_h) + Y_b \quad (1)$$

where the first term is the Bragg scattering, containing a scale factor  $S$ , a correction factor  $K$ , a structure factor  $F_h$ , and a profile function  $P(\Delta T_h)$ , as determined by the displacement  $\Delta T_h$  of the profile point from the reflection position, and the second term  $Y_b$  is the background intensity. The sum is over all profile points in all the scans included in the refinements. Within the correction factor  $K$  in equation (1) is a term which describes the change in intensity for a Bragg reflection due to texture<sup>15-23</sup>.

### Rietveld Quantitative Analysis

The advantages of the Rietveld method<sup>8-14</sup> for quantitative phase analysis<sup>3-7</sup> of the XRD data of the many identified phases or mixtures are —

- The calibration constants are computed from simple literature data (i.e.,  $Z$ ,  $M$ , and  $V$  values) rather than by laborious experimentation,
- All reflections in the pattern are explicitly included, irrespective of overlap,
- The background is better defined since a continuous function is fitted to the whole powder diffraction pattern,
- The preferred orientation effects can be corrected and determined, and
- The crystal structural and peak-profile parameter scan be refined as part of the same analysis.

Therefore, the Rietveld quantitative analysis<sup>3-7</sup> has been used world-widely to determine the weight percentage for each of the identified phases without the need for laborious experimental calibration procedures. The right starting crystallographic information file (e.g., space group, cell parameters, atomic positions, etc.) of each phase in a mixture is required for this Rietveld quantitative analysis method<sup>3-7</sup>. The crystallographic information file can be obtained from the International Crystal Structure Data (ICSD) and ICDD. The percentage for each of the identified phases of XRD data of deposits is proportional to the product of the scale factor ( $s_p$ ), as derived in a multiphase Rietveld analysis of the XRD pattern (see equation 2), with the mass ( $M$ ) and volume ( $V$ ) of the unit cell. If all phases are identified and crystalline which means that there is no amorphous materials, the weight percentage  $W$  of phase  $p$  is given by:

$$W_p = s_p (ZMV)_p / \sum_{i=1}^n s_i (ZMV)_i \quad (2)$$

Where  $s$  is the Rietveld scale factor,  $Z$  is the number of formula units per unit cell,  $M$  is the mass of the formula unit, and  $V$  is the unit cell volume (in  $\text{\AA}^3$ ) for each of the identified phases of XRD data of deposits.

In this study, the crystal structure refinement, phase composition (i.e., Rietveld quantitative analysis) and texture for each phase of scale and corrosion deposits formed in the equipment parts of refineries and gas plants, which is an important industrial challenge for the analysts, were determined using the Rietveld program<sup>24</sup> with the generalized spherical harmonics description<sup>15,18,20-23</sup> for preferred crystallographic orientation correction.

## EXPERIMENTAL

### Sample Preparation

The nature of the starting scale and corrosion deposits investigated at the present study were—

- Crystal structures, crystallographic preferred orientations refinement<sup>15-23</sup> and quantitative phase analysis<sup>3-7</sup> of XRD data of corrosion deposits in the form of oxide corrosion products such as magnetite [Fe<sub>3</sub>O<sub>4</sub>], hematite [Fe<sub>2</sub>O<sub>3</sub>] and goethite [FeOOH] from the boiler equipment parts in the gas plant,
- Quantitative phase analysis of synthetic mixtures of drilling mud in the form of barium sulfate (87 wt% of barite-BaSO<sub>4</sub>), formation material in the form of silicon oxide (8 wt% of quartz-SiO<sub>2</sub>) and iron oxide corrosion products (5 wt% of hematite-Fe<sub>2</sub>O<sub>3</sub>) and
- Quantitative phase analysis of sludge deposits that were collected from the equipment parts in a refinery.

The starting materials were considered to be excellent for this study because a high-quality crystal structure of iron oxide (magnetite, hematite, and goethite), barite<sup>25</sup> and quartz<sup>26</sup> have been reported in the literature. The starting scale and corrosion deposits were manually ground in an agate mortar and a pestle for several minutes to achieve fine particle size<sup>22</sup>. Then, the fine scale and corrosion deposits mounted into the XRD sample holder by front pressing.

### XRD Data Measurements and Rietveld Calculations

Step-scanned patterns were measured with an X-ray powder diffractometer (Rigaku Ultima IV) with a copper X-ray tube ( $\lambda=1.5406 \text{ \AA}$ ). A monochromator and a proportional detector were used in conjunction with a  $0.67^\circ$  divergence slit, a  $0.67^\circ$  scattering slit, and a 0.3-mm receiving slit at instrument settings of 40 kV and 40 mA. The XRD data were measured from  $10^\circ$  to  $140^\circ$  in  $2\theta$  Bragg-angle, using a step size of  $0.04^\circ$  and a counting time of  $1^\circ$  per minute<sup>2,27-29</sup>. Then, the software package<sup>13</sup> (High Score Plus version 3.0e, PANalytical B.V.), combined with the ICDD and PDF-4+ database of the standard reference materials, was used for the phase identification (i.e., qualitative analysis) of XRD data of scale and corrosion deposits.

The least-squares structure and profile refinements of XRD data were performed with Rietveld refinement program<sup>24</sup>. The structural models (i.e., crystallographic information file) used for the scale deposits, corrosion deposits, barite, and quartz were taken from the ICSD. The refined parameters were similar to those described by Sitepu et al.<sup>22</sup>, and are the following: phase scale factors, Chebychev polynomial background parameters, lattice parameters, the instrument zero-point, atomic isotropic and anisotropic displacement coefficients, the Lorentzian and the Gaussian terms of a pseudo-Voigt profile function, and the generalized spherical harmonics description for the crystallographic preferred orientation correction. The results of crystallographic information, such as crystal structure, phase composition, and crystallographic preferred orientation obtained from Rietveld refinement for all the XRD data sets, are given in the next section.

## RESULTS AND DISCUSSIONS

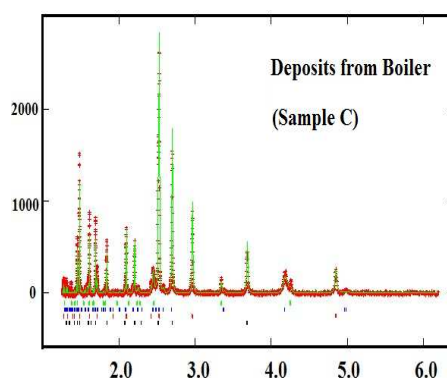
### The Deposits Collected from the Boiler Equipment in Gas Plant

The agreement between the calculated and measured XRD patterns following Rietveld refinement with the generalized spherical harmonic description for the corrosion deposits in the form of magnetite [ $\text{Fe}_3\text{O}_4$ ], hematite [ $\text{Fe}_2\text{O}_3$ ], goethite [ $\text{FeO}(\text{OH})$ ], and the formation material in the form of silicon oxide [*i.e.*, quartz ( $\text{SiO}_2$ )] are given in Figure 1(a). The observed data are indicated by plus sign and the calculated profile is the solid line in the same field. The sets of vertical lines below the profiles represent the positions of all possible Bragg reflections for the iron oxide corrosion products in the form of magnetite [ $\text{Fe}_3\text{O}_4$ ], hematite [ $\text{Fe}_2\text{O}_3$ ], goethite [ $\text{FeO}(\text{OH})$ ], and formation material normally found in the sandstone or sand in the form of quartz [ $\text{SiO}_2$ ] phases. The refined structural parameters for the identified phases — magnetite [ $\text{Fe}_3\text{O}_4$ ], hematite [ $\text{Fe}_2\text{O}_3$ ], goethite [ $\text{FeO}(\text{OH})$ ], and silicon oxide [*i.e.*, quartz ( $\text{SiO}_2$ )] phases agreed well with the corresponding results reported in the literature.

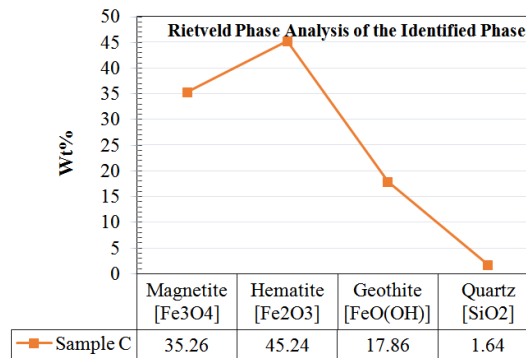
Figure 1(b) shows the variation in the quantitative phase analysis or weight percentage (wt%) obtained from Rietveld refinement with March model for crystallographic preferred orientation correction with the identified phases. It can be seen from the Figure that 98.36 wt% of iron oxide corrosion product in the form of 45.24 wt% of hematite [ $\text{Fe}_2\text{O}_3$ ], 35.26 wt% of magnetite [ $\text{Fe}_3\text{O}_4$ ], 17.86 wt% of goethite [ $\text{FeO}(\text{OH})$ ] phases for the corrosion deposit, with the additional of the 1.64 wt% of the sandstone or sand in the form of quartz [ $\text{SiO}_2$ ] phase.

Figure 2 shows the variation between the preferred crystallographic orientation correction factor (or pole density distribution function) and the orientation angle both for corrosion product in the form of the  $\langle 001 \rangle$  magnetite [ $\text{Fe}_3\text{O}_4$ ] and  $\langle 001 \rangle$  hematite [ $\text{Fe}_2\text{O}_3$ ] obtained from Rietveld refinement with the generalized spherical harmonic description. Note that, the pole density distribution function is unity in case of the corrosion deposits are randomly oriented, and yields no variation between the crystallographic orientation correction factor and the orientation angle (*i.e.*, straight line).

It can be seen clearly from Figure 2 that the crystallographic preferred orientation correction factors of the corrosion deposits in the form of the  $\langle 001 \rangle$  magnetite [ $\text{Fe}_3\text{O}_4$ ] phase is higher than that of the corresponding value for the corrosion deposits in the form of the  $\langle 001 \rangle$  hematite [ $\text{Fe}_2\text{O}_3$ ], indicating that the deposits are pronounced crystallographic preferred orientation (or texture of crystalline materials). Therefore, the XRD intensities of the corrosion deposits have to be corrected due to the preferred orientation by using the Rietveld refinement with the generalized spherical harmonics description both for the quantitative phase analysis (phase composition) and crystal structure refinement.



(a). Rietveld Fit



(b). Rietveld Phase Analysis for Each of the Identified Phases

Figure 1: (a) The Agreement Between the Calculated and Measured XRD Patterns from 0.6 Å to 6.0 Å of the d-spacings (Horizontal) for the Corrosion Deposits from Boiler following Rietveld Refinement with Generalized Spherical Harmonics Description for Preferred Orientation Correction. (b) Variation Between the Weight Percentage (wt%) Obtained from Rietveld Refinement with the Generalized Spherical Harmonics Description for Crystallographic Preferred Orientation Correction and the Identified Phases for Corrosion Deposits from the Specific Boiler Equipment in the Gas Plant.

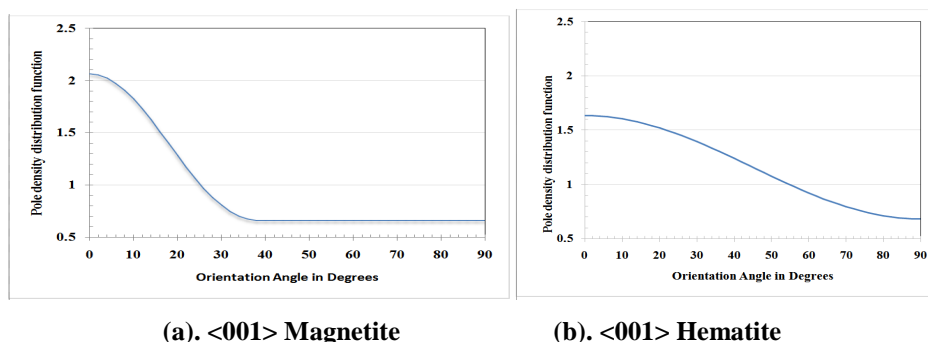


Figure 2: The Variation Between the March Preferred Orientation Corrections with Orientation Angle Derived from Rietveld Refinement with the March Model—for (a) the <001> Magnetite [Fe<sub>3</sub>O<sub>4</sub>] and (b) the <001> Hematite [Fe<sub>2</sub>O<sub>3</sub>].

### The Synthetic Mixed of Barite, Quartz, and Hematite Powders

In addition to iron oxide in the form of hematite [Fe<sub>2</sub>O<sub>3</sub>], the formation material in the form of silicon oxide [e.g., quartz (SiO<sub>2</sub>)] with the ICDD PDF number 01-077-1060 appears in almost all of the corrosion products and, therefore it has been included in the present study. Additionally, the mineral barite [e.g., barium sulfate (BaSO<sub>4</sub>)] is used in the oil drilling industry for lubrication and, therefore it is of interest primarily in materials characterization research. Noted, that, the deposits from the equipment at refineries and gas plants sometimes also consist of barite, and, therefore, it is included in this study. The density and color of this natural mineral make it a valuable product. In each application, the purity and composition of the contaminants should be closely monitored as they may alter the properties and function of the material.

The authors extended the above work for the synthetic mixed of barite, quartz and hematite powder to perform Rietveld quantitative analysis of the known mixture of barite, quartz, and hematite to test the reliability and reproducibility of the Rietveld refinement with the generalized spherical harmonics description for preferred orientation correction factor.

The weight percentages (wt%) of the known mixture were prepared by—barite(87 wt%), quartz (8wt%), and hematite (5wt%). The phase composition results obtained from Rietveld refinement with the generalized spherical harmonics description were 87.8(7) wt% for barite, 8.7(6) wt% for quartz, and 3.5(5) wt% for hematite, respectively, which agreed well with the known values. The number in parentheses gives the estimated standard uncertainty for the least significant figure of the parameter. Additionally, the refined crystal structure parameters agreed well with the results reported in the literature, see Table 1. Therefore, it can be summarized that the Rietveld refinement with the generalized spherical harmonics description for crystallographic preferred orientation correction in XRD analysis yields accurate, reliable, and reproducibility results for both crystal structure refinement and quantitative analysis of the investigated deposits.

### Quantitative Phase Analysis of Sludge Deposits that were Collected from the Equipment Parts in a Refinery

The sludge deposits that frequently accumulate inside the equipment used in the oil industry can cause failures and temporarily shut down the refinery and gas plants. In this study, a new sample preparation method developed by Sitepu, Al-Ghamdi and Zaidi (2018)<sup>2,28-29</sup> was extended and assessed to separate the inorganic materials (i.e., non-hydrocarbon part) from the hydrocarbon (dichloromethane soluble part) of the sludge deposits that were collected from the equipment parts in a refinery. Rietveld refinement of the X-ray powder diffraction (XRD) data for all of the identified phases showed that the very small quantities of inorganic materials (i.e., non-hydrocarbon part) of the sludge deposits consisted mainly of 82 wt% of iron oxide corrosion products in the form of 56 wt% of goethite [FeO(OH)], 15wt% of magnetite [Fe<sub>3</sub>O<sub>4</sub>] and 11wt% of lepidocrocite [FeO(OH)], 16 wt% of iron sulfide corrosion products in the form of 15 wt% of pyrite [FeS<sub>2</sub>] and 1 wt% of pyrrhotite [Fe<sub>7</sub>S<sub>8</sub>], and formation materials in the form of 2 wt% of quartz [SiO<sub>2</sub>], Figure 3. Table 2 showed the relationship between their XRD phase identification results of the sludge samples that were generated in the particular equipment in refineries and gas plants and the nature of the corrosion and scale products.

**Table 1: Summary of Refined Structure Parameters and Weight Percentage (wt%) Results for the Synthetic Mixture of 87 wt% of Barite, 8 wt% of Quartz and 5 wt% of Hematite Obtained from Rietveld Refinement with the Generalized Spherical Harmonics Description**

Refined Parameters	This Study	Single Crystal XRD Data <sup>25</sup>
<b>Barite [e.g., Barium sulfate(BaSO<sub>4</sub>)]</b>		
Ba(x,y,1/4)		
x	0.1581(4)	0.15842(2)
y	0.1848(3)	0.18453(2)
U	0.0149(5)	0.011(4)
S(x,y,3/4)		
x	0.192(1)	0.19082(9)
y	0.433(1)	0.43749(7)
U	0.020(1)	0.009(9)
O1(x,y,3/4)		
x	0.134(3)	0.1072(4)
y	0.578(3)	0.5870(3)
U	0.0165	0.023(5)
O2(x,y,3/4)		
x	0.032(4)	0.0498(3)
y	0.313(3)	0.3176(2)
U	0.0165	0.018(6)
O3(x,y,z)		

Table 1 Contd.,		
x	0.314(2)	0.3118(2)
y	0.407(2)	0.4194(2)
z	0.944(3)	0.9704(2)
U	0.0165	0.013(2)
<b>Quartz [e.g., silicon oxide (SiO<sub>2</sub>)]</b>		
Si(x,0,1/3)		
x	0.58(1)	0.53013
U	0.056	0.056
O(x,y,z)		
x	0.385(9)	0.4141
y	0.14(2)	0.1460
z	0.11(1)	0.1188
U	0.096	0.096
<b>Hematite [e.g., iron oxide (Fe<sub>2</sub>O<sub>3</sub>)]</b>		
Fe(0,0,z)		
z	0.150(3)	0.1447
U	0.05	0.05
O(x,0,1/4)		
x	0.31(2)	0.3059
U	0.07	0.07
<b>Known Weight Percentage (wt%)</b>		
87 wt% of Barite (BaSO <sub>4</sub> )	87.8(7)	
8wt% of Quartz (SiO <sub>2</sub> )	8.7(6)	
5 wt% of Hematite (Fe <sub>2</sub> O <sub>3</sub> )	3.5(5)	

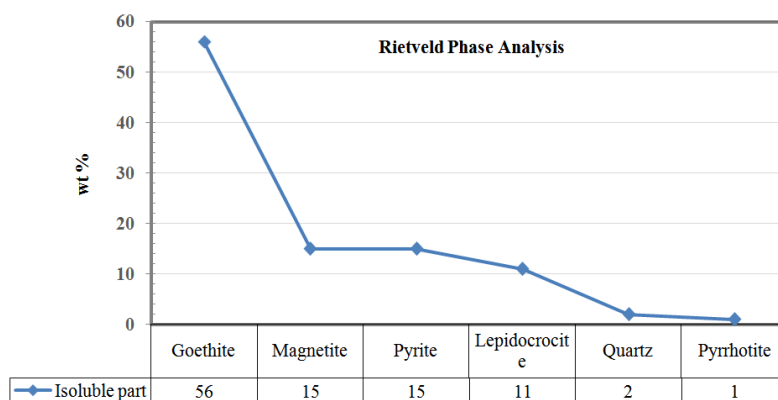


**Figure 3: Variation Between the Weight Percentage (wt%) and the Identified Phases for Corrosion Deposits from the Specific Boiler Equipment in Gas Plant Obtained from Rietveld Refinement with the Generalized Spherical Harmonics Description for Crystallographic Preferred Orientation Correction.**

**Table 2: Summary of the Identified Phases of the Very Small Quantities of Inorganic Materials (Non-Hydrocarbon) and its Nature of the Deposits from Equipment Parts in Refineries and Gas Plants**

The Identified Phases of the Very Small Quantities of Inorganic Materials (Non-Hydrocarbon Part)	Nature of the Corrosion and Scale Products
Magnetite (Fe <sub>3</sub> O <sub>4</sub> ), Lepidocrocite (FeOOH), Goethite (FeOOH), and Akaganeite (FeOOH)	Iron Oxide Corrosion Product - at a high-temperature magnetite corrosion products it will coat the iron/steel to prevent oxygen to reach underlying metal. Mostly, at low temperature, lepidocrocite formed and with time it transformed into most stable goethite. Akaganeite formed in marine environments.
Greigite (Fe <sub>3</sub> S <sub>4</sub> ), Pyrite (FeS <sub>2</sub> ), Marcasite (FeS <sub>2</sub> ), Mackinawite (FeS <sub>0.9</sub> ), and Pyrrhotite (Fe <sub>7</sub> S <sub>8</sub> )	Iron Sulfide Corrosion Products - pyrophoric iron sulfide (pyrrhotite-FeS) results from the corrosive action of sulfur or sulfur compounds (H <sub>2</sub> S) on the iron (steel) and moisture.
Iron Chloride (FeCl <sub>3</sub> ), and Iron Chloride Hydrate (FeCl <sub>2</sub> ·4H <sub>2</sub> O)	Chloride corrosion products
Calcite (CaCO <sub>3</sub> ), Aragonite (CaCO <sub>3</sub> ), and Siderite (FeCO <sub>3</sub> )	Carbonate scale
Basanite (CaSO <sub>4</sub> ·2H <sub>2</sub> O), Anhydrite (CaSO <sub>4</sub> ), and Gypsum (CaSO <sub>4</sub> ·2H <sub>2</sub> O)	Sulfate scale
Quartz (SiO <sub>2</sub> ), Albite (NaAlSi <sub>3</sub> O <sub>8</sub> ), Microcline (KAlSi <sub>3</sub> O <sub>8</sub> ), and Cristoballite (SiO <sub>2</sub> )	Formation material - Normally found in the sandstone or sand
Illite (K <sub>0.5</sub> (AlFeMg) <sub>3</sub> (SiAl) <sub>4</sub> O <sub>10</sub> (OH) <sub>2</sub> )	Clay minerals normally found with sandstone
Ettringite (Ca <sub>6</sub> Al <sub>2</sub> (SO <sub>4</sub> ) <sub>3</sub> (OH) <sub>12</sub> )	Cementing material
Barite (BaSO <sub>4</sub> )	Drilling mud
Aluminum Oxide (Al <sub>2</sub> O <sub>3</sub> )	Normally from the catalyst
Sulfur (S)	
Sodium Iron Oxide (NaFeO <sub>2</sub> )	

## CONCLUSIONS

In the present study, the authors described the Rietveld refinement of the all XRD data sets for the — corrosion deposits from the boiler, and the additional of synthetic mixtures of drilling mud in the form of barium sulfate [barite(BaSO<sub>4</sub>)], formation material in the form of silicon oxide [quartz(SiO<sub>2</sub>)] and iron oxide [hematite(Fe<sub>2</sub>O<sub>3</sub>)] with the weight percentage (wt%) of 87wt% of barite [BaSO<sub>4</sub>], 8 wt% of silicon oxide [quartz(SiO<sub>2</sub>)] and 5 wt% of hematite [Fe<sub>2</sub>O<sub>3</sub>]. Based on the results, it can be concluded that: —

- Good agreement between the measured and calculated XRD patterns of all samples when the generalized spherical harmonic description was used to correct the intensities due to the effects of preferred orientation;
- The refined structural parameters agreed well with the XRD single crystal results reported in the literature;
- Rietveld quantitative analysis results for the synthetic mixtures of barite, quartz, and hematite that were prepared independently agreed well with the known weight percentage of the mixture samples, which indicate that the Rietveld refinement yields the reproducibility of the structural and quantitative phase analysis results.

It can therefore, be summarized that the Rietveld refinement with the March model for preferred orientation correction in XRD data of scale and corrosion deposits and synthetic mixture powders yields accurate, reliable, and reproducibility results for both crystal structure refinement and quantitative analysis of the investigated deposits from the refinery and gas plants. Knowing quantitatively the findings which structure, texture, and compositions for each phase were involved in the scale formation and corrosion deposits can help the field engineers to take preventive action to stop the generation of those particular deposits.

## ACKNOWLEDGEMENTS

The authors would like to acknowledge Saudi Aramcomanagement for giving permission to publish the results. Mr. Yazeed A. Al-DukhayyilandMr. Mossad A. Al-Fahadis acknowledged for their support in this study. Thanks are also due to Dr. ShouwenShen for his help in encouraging one of the authors(H.S) to extend H.S's previous excellent crystallography research on Rietveld refinement of whole X-rays, synchrotron and neutron powder diffraction data for quantitatively determining the crystal structure, texture and quantitative phase analysis (wt%) of the unknown deposits generated in in refineries and gas plants.

## REFERENCES

1. Smith, S.N.: "Corrosion Product Analysis in Oil and Gas Pipelines," *Chemical Treatment*, July 7, 2004.
2. Sitepu, H. Al-Ghamdi, R.A. and Zaidi, S.R.: "Corrigendum for Application of a New Method in Identifying the Sludge Deposits from Refineries and Gas Plants: A Case of Laboratory-Based Study," *International Journal of Corrosion*, Volume 2018, (Article ID 8646104), 1 page <https://doi.org/10.1155/2018/8646104>.
3. Hill, R.J. and Howard, C.J.: "Quantitative Phase Analysis from Neutron Powder Diffraction Data Using the Rietveld Method," *Journal of Applied Crystallography*, Vol. 20, 1987, pp. 467-474.
4. O'Connor, B.H. and Raven, M.D.: "Application of the Rietveld Refinement Procedure in Assaying Powdered Mixtures," *Powder Diffraction Journal*, Vol. 3, No. 4, 1988, pp. 2-6.
5. Bish, D.L. and Howard, S.A.: "Quantitative Phase Analysis Using the Rietveld Method," *Journal of Applied Crystallography*, Vol.21, 1988, pp. 86-91.
6. Giannini, C., Guagliardi, A. and Millin, R.: "Quantitative Phase Analysis by Combining the Rietveld and the Whole-Pattern Decomposition Methods," *Journal of Applied Crystallography*, Vol. 35, Issue 4, August 2002, pp. 481-491.
7. Scarlett, N.V.Y. and Madsen, I.C.: "Quantification of Phases with Partial Or No Known Crystal Structure," *Powder Diffraction Journal*, Vol. 21, Issue 4, March 2006, pp. 278-284.
8. Rietveld, H.M.: "A Profile Refinement Method for Nuclear and Magnetic Structures," *Journal of Applied Crystallography*, Vol. 2, Issue 2, June 1969, pp. 65-71.
9. Young R.A.: *The Rietveld Method*, International Union of Crystallography. Oxford University Press, Oxford, United Kingdom, 1995. 298 p.

10. Mccusker, L.B., Von Dreele, R.B., Cox, D.E., Louer, D. and Scardi, P. "Rietveld refinement guidelines," *Journal of Applied Crystallography*, Vol. 32, Issue 1, February 1999, pp. 36–50.
11. Toby, B.H. and Von Dreele, R.B. "GSAS-II: The Genesis of a Modern Open-Source All Purpose Crystallography Software Package," *Journal of Applied Crystallography*, Vol. 46, Issue 2, April 2013, pp. 544-549.
12. Toby, B.H. and Von Dreele, R.B. "What's new in GSAS-II," *Powder Diffraction Journal*, Vol. 29, Issue S2, December 2014, pp. S2-S6.
13. Degen, T., Sadki, M., Bron, E., König, U. and Nénert, G. "The HighScore Suite," *Powder Diffraction Journal*, Vol. 29, Issue S2, December 2014, pp. S13-S18.
14. Hewat, A., David, W.I.F. and van Eijck, L.: "Hugo Rietveld (1932-2016)," *Journal of Applied Crystallography*, Vol. 49, Issue 4, August 2016, pp. 1394-1395.
15. Bunge, H.J.: "Texture Analysis in Materials Science: Mathematical Methods," Butterworths-Heinemann, London, 1982.
16. Dollase, W.A.: "Correction of Intensities for Preferred Orientation in Powder Diffractometry: Application of the March Model," *Journal of Applied Crystallography*, Vol. 19, Issue 4, August 1986, pp. 267-272.
17. O'Connor, B.H., Li, D.Y. and Sitepu, H.: "Strategies for Preferred Orientation Corrections in X-ray Powder Diffraction Using Line Intensity Ratios," *Advances in X-ray Analysis*, Vol. 34, 1991, pp. 409-415.
18. Popa, N.C.: "Texture in Rietveld Refinement," *Journal of Applied Crystallography*, Vol. 25, Issue 5, October 1992, pp. 611-616.
19. O'Connor, B.H., Li, D.Y. and Sitepu, H.: "Texture Characterization in X-ray Powder Diffraction Using the March Formula," *Advances in X-ray Analysis*, Vol. 35, 1992, pp. 277-283.
20. Järvinen, M.: "Application of Symmetrized Harmonics Expansion to Correction of the Preferred Orientation Effect," *Journal of Applied Crystallography*, Vol. 26, 1993, pp. 525-531.
21. Von Dreele, R.B.: "Quantitative Texture Analysis by Rietveld Refinement," *Journal of Applied Crystallography*, Vol. 30, Issue 4, August 1997, pp. 517-525.
22. Sitepu, H., O'Connor, B.H. and Li, D.Y.: "Comparative Evaluation of the March and Generalized Spherical Harmonic Preferred Orientation Models Using X-ray Diffraction Data for Molybdenite and Calcite Powders," *Journal of Applied Crystallography*, Vol. 38, Issue 1, February 2005, pp. 158-167.
23. Sitepu, H.: "Texture and Structural Refinement Using Neutron Diffraction Data from Molybdenite ( $\text{MoO}_3$ ) and Calcite ( $\text{CaCO}_3$ ) Powders and a Ni-rich  $\text{Ni}_{50.7}\text{Ti}_{49.30}$  Alloy," *Powder Diffraction Journal*, Vol. 24, Issue 4, December 2009, pp. 315-326
24. Larson, A.C. and Von Dreele, R.B.: "General Structure Analysis System (GSAS)," Report LAUR 86-748, Los Alamos, New Mexico: Los Alamos National Laboratory, 2000.

25. Jacobsen, S. D., Smyth, J. R., Swope, R. J., Downs, R.T.: "Rigid-body character of the SO<sub>4</sub> groups in celestine, anglesite and barite", *Canadian Mineralogist*, Vol. 36, 1998, pp. 1053-106.
26. Antao, S.M., Hassan, I., Wang, J., Lee, L.P. and Toby, B.H.: "State-of-the-Art High-Resolution Powder X-ray Diffraction (HRPXR) Illustrated with Rietveld Structure Refinement of Quartz, Sodalite, Tremolite and Meionite," *Canadian Mineralogist*, Vol. 46, 2008, pp. 1501-1509.
27. Al-Sharidi, S.H., Sitepu, H. and AlYami, N.M.: "Application of Tungsten Oxide (WO<sub>3</sub>) Catalysts Loaded with Ru and Pt Metals to Remove MTBE from Contaminated Water: A Case Of Laboratory-Based Study," *IMPACT: International Journal of Research in Engineering & Technology*, ISSN (P): 2347-4599; ISSN (E): 2321-8843; Vol. 6, Issue 8, Aug 2018, 19-30.
28. Sitepu, H. Al-Ghamdi, R.A. and Zaidi, S.R.: "Application of a New Method in Identifying the Sludge Deposits from Refineries and Gas Plants: A Case of Laboratory-Based Study," *International Journal of Corrosion*, Volume 2017, Article ID 9047545, 7 pages, <https://doi.org/10.1155/2017/9047545>.
29. Al-Ghamdi, R.A. and Sitepu, H.: "Characterization of Sludge Deposits from Refineries and Gas Plants: A Prerequisite Results Requirements to Facilitate Chemical Cleaning of the Particular Equipment," *International Journal of Corrosion* 2018. (Article ID 4121506), 9 page. <https://doi.org/10.1155/2018/4121506>.